HUMAN VISUAL SYSTEM BASED MULTI-HISTOGRAM EQUALIZATION FOR NON-UNIFORM ILLUMINATION AND SHOADOW CORRECTION

Eric Wharton[a], Dr. Karen Panetta[a], Dr. Sos Agaian[b]

[a]Tufts University, Department of Electrical and Computer Engineering, Medford, MA 02155
[b]The University of Texas at San Antonio, 6900 North Loop 1604 West, San Antonio, TX 78249

ABSTRACT

Images that do not have uniform brightness pose a challenging problem for image enhancement systems. As histogram equalization has been successfully used to correct for uniform brightness problems, we propose a new histogram equalization method that utilizes human visual system based thresholding as well as logarithmic processing techniques. Whereas previous histogram equalization methods have been limited in their ability to enhance these images, we will demonstrate the effectiveness of this new method by enhancing a range of images with shadowing effects and inconsistent illumination. The images shown will include images captured professionally and with cell phone cameras. Comparison with other methods will be presented

Index Terms— Image Enhancement, Human Visual System, Logarithmic Arithmetic, Histogram Equalization

1. INTRODUCTION

In this paper, we introduce the human visual system based multi-histogram equalization method. This algorithm capitalizes on the advantages of multi-histogram equalization with the benefit of an effective quantitative measure to ensure optimal results as well as local histogram equalization while removing useless information to avoid the production of artifacts. We compare the results of the proposed algorithm against the results of the leading adaptive and local algorithms on a large number of images, presenting a representative collection. This demonstrates the effectiveness of the human vision based multi-histogram equalization algorithm.

Histogram equalization and its variations are outlined in [1][2][3][4][5]. These papers also identify deficiencies with the algorithms, such as the introduction of artifacts or over-enhancement of regions. Further, experimental results show that these methods are unable to correct for non-uniform illumination and shadows. Local, or adaptive, histogram equalization divides the image into semi-overlapping blocks and equalizes these blocks separately.

Multi-histogram equalization has generally been limited to bi-histogram equalization, and previous results have shown tri-histogram equalization to have no consistent advantage. In this paper, we demonstrate a method that overcomes this limitation by separating the image into different regions of illumination instead of thresholding by simple pixel intensity. In this manner, histogram equalization can be used on each region to correct for non-uniform illumination. In order to perform this segmentation, we utilize the model of the human visual system.

This paper is organized as follows: Section 2 presents background information. Section 3 will present the methods. Section 4 will present the results of computer simulations. Section 5 will be a discussion of results and some concluding comments are made.

2. BACKGROUND

In this section, we provide a brief description of the standard histogram equalization algorithm, the Logarithmic Image Processing (LIP) model, and the Logarithmic AME performance measure.

2.1. Histogram Equalization

Standard histogram equalization uses a cumulative density function to attempt to force a uniform probability density function for an image, remapping the pixel intensities according to the following formula:

$$f(x) = Y_{\min} + (Y_{\max} - Y_{\min}) \cdot P(x) \qquad (1)$$

Where *f(x)* is the pixel intensity of the output image, x is the pixel intensity of the input image, Y_{max} and Y_{min} are the desired maximum and minimum for the output range, respectively, and *P(x)* is the cumulative density, where $P(X_{max}) = 1$.

This can then be modified into a local method. Adaptive, or local, histogram equalization divides the image into partially overlapping blocks which are then equalized separately and averaged. Generally, using more windows gives a better quality enhancement at the cost of computational and time complexity.

This can also be modified into bi-histogram equalization. This is done by splitting the image into two

(a) (b) (c) (g)

Figure 1. Bed image enhanced using the variants of histogram equalization; (a)Original bed image, bed image enhanced using (b)dualistic sub-image histogram equalization, (c)minimum mean brightness error bi-histogram equalization, (d)bi-histogram equalization with parameters chosen using the Logarithmic AME

sub-images based on a threshold, with all values above the threshold in one image and all those below in the other. The two images are then equalized separately and recombined. Many attempts have been made to define the optimal value of this threshold. However, as no enhancement measure has been used, these methods can be improved upon. Figure 1 compares the results of several of these methods to the results using the Logarithmic AME measure of image enhancement.

2.2. Logarithmic Image Processing (LIP) model

The LIP model was introduced by Jourlin and Pinoli to give a non-linear framework for image processing [6]. This is designed to both maintain the pixel values inside the range [0,M) as well as to more accurately process images from a human visual system point of view. The LIP model can be summarized as follows:

$$a \oplus b = a + b - \frac{ab}{M} \tag{2}$$

$$a \Theta b = M\,\frac{a-b}{M-g} \tag{3}$$

$$c \otimes a = M - M\left(1 - \frac{f}{M}\right)^{c} \tag{4}$$

$$a * b = \varphi^{-1}\left(\varphi(a)\cdot\varphi(b)\right) \tag{5}$$

Where we use $\oplus$ as LIP addition, Θ as LIP subtraction, $\otimes$ as LIP scalar multiplication, and * as LIP grayscale multiplication. Also, *a* and *b* are any grey tone pixel values, is the maximum value of the range, and *c* is a constant. In general, *a* and *b* correspond to the same pixel in two different images that are being added, subtracted, or multiplied. For the grayscale multiplication, the functions φ and φ^{-1} are defined as:

$$\varphi(a) = -M \cdot \ln\left(1 - \frac{f}{M}\right) \tag{6}$$

$$\varphi^{-1}(a) = M \cdot \left[1 - \exp\left(\frac{-f}{M}\right)\right] \tag{7}$$

Where α and β are user-defined operating parameters which can be fine-tuned for the specific images being processed [8].

2.3. Measure of Image Enhancement

A problem of image enhancement has always been to develop a quantitative measure to assess image enhancement. The Logarithmic AME and Logarithmic AMEE measures utilize the Michelson Contrast as well as Fisher's Law or Entropy [7]. The measures function by segmenting an image into *k1 x k2* sized blocks, assessing each block separately according to the following formulae, and averaging the results.

$$\log AME_{k_1k_2}(\Phi) = \frac{1}{k_1k_2} \otimes \sum_{i=1}^{k_1}\sum_{j=1}^{k_2} \frac{1}{20} \otimes \ln\left(\frac{I^w_{\max:k,l}\Theta I^w_{\min:k,l}}{I^w_{\max:k,l} \oplus I^w_{\min:k,l}}\right) \tag{8}$$

$$\log AMEE_{k_1k_2}(\Phi) = \frac{1}{k_1k_2} \otimes \sum_{i=1}^{k_1}\sum_{j=1}^{k_2} \frac{I^w_{\max:k,l}\Theta I^w_{\min:k,l}}{I^w_{\max:k,l} \oplus I^w_{\min:k,l}} * \ln\left(\frac{I^w_{\max:k,l}\Theta I^w_{\min:k,l}}{I^w_{\max:k,l} \oplus I^w_{\min:k,l}}\right) \tag{9}$$

Where $I^w_{\max;k,l}$ and $I^w_{\min;k,l}$ are the local maximum and minimum, respectively. The summations use LIP arithmetic.

It is important to note that this method is relative. This means that it is not an arbitrary standard of "goodness," but rather a means of comparing similarly processed images. Further, larger or smaller numbers are not necessarily better, instead this depends on the image.

3. METHODS

In this section, we present the human vision thresholding (HVT) algorithm and the multi-histogram equalization using HVT method.

3.1. Human Visual System Based Image Enhancement

Human Visual System (HVS) based Image Enhancement aims to emulate the way in which the human visual system discriminates between useful and useless data [8] and is based on the background illumination and the gradient. The former is arrived at using the following formula:

$$B(x,y)=\left[\frac{1}{2}\left(\frac{1}{4}\sum_{Q}X(i,j)+\frac{1}{4\sqrt{2}}\sum_{Q'}X(k,l)\right)+X(x,y)\right]\div 2 \tag{10}$$

Where $B(x,y)$ is the background intensity at each pixel, $X(x,y)$ is the input image, Q is all of the pixels which are directly up, down, left, and right from the pixel, and Q' is all of the pixels diagonally one pixel away. We must also define a parameter B_T, which is the maximum difference in the image, arrived at using:

$$B_T=\max(X(x,y))-\min(X(x,y)) \tag{11}$$

Further, the gradient information is needed, which is arrived at in the following formula:

$$G_1=X(x,y)-X(x,y+1) \qquad G_2=X(x,y)-X(x+1,y) \qquad X'(x,y)=(|G_1|+|G_2|)\div 2 \tag{12}$$

where $X'(x,y)$ is the gradient information and G_1, G_2 are the directional gradients. Finally, we must also know some parameters concerning the human eye itself, which we will call B_{xi}, I = 1,2,3 and K_i, I = 1,2,3. These are arrived at using the following formulas:

$$\begin{aligned}B_{x1}&=\alpha_1 B_T\\ B_{x2}&=\alpha_2 B_T\\ B_{x3}&=\alpha_3 B_T\end{aligned} \tag{13}$$

$$\begin{aligned}K_1&=\frac{1}{100}\beta\cdot\max\left(\frac{X'(x,y)}{B(x,y)}\right)\\ K_2&=K_1\sqrt{B_{x2}}\\ K_3&=K_1/B_{x3}\end{aligned} \tag{14}$$

Where α_1, α_2, α_3 are parameters based upon the three different regions of response characteristics displayed by the human eye. As α_1 is the lower saturation level, it is effective to set this to 0. For α_2, α_3, it is necessary to determine these experimentally, or using the measure.

Using this information, the image is first broken up into the different regions of human visual response. These different regions are characterized by the minimum difference between two pixel intensities for the human visual system to register a difference. Next, these three regions are thresholded, removing the pixels which do not constitute a noticeable change for a human observer and placing these in a fourth image. These four images are arrived at using the following formula:

$$\begin{aligned}&\mathrm{Im}1=X(x,y) && && B_{x2}\geq B(x,y)\geq B_{x1}\ \&\ \frac{X'(x,y)}{\sqrt{B(x,y)}}\geq K_2\\ &\mathrm{Im}2=X(x,y) && \text{such that} && B_{x3}\geq B(x,y)\geq B_{x2}\ \&\ \frac{X'(x,y)}{B(x,y)}\geq K_1\\ &\mathrm{Im}3=X(x,y) && && B(x,y)\geq B_{x3}\ \&\ \frac{X'(x,y)}{B(x,y)^2}\geq K_3\\ &\mathrm{Im}4=X(x,y) && && \text{All Remaining Pixels}\end{aligned} \tag{15}$$

These four images are then enhanced separately and recombined to form the enhanced image.

3.1. HVS Based Multi-Histogram Equalization

Experimental results have shown no significant improvement between tri-histogram equalization using the standard thresholding method and bi-histogram equalization. Another method is necessary to achieve better results using multi-histogram equalization.

By separating the image into regions by the quality of illumination, such as over-illuminated, well illuminated, and under-illuminated, traditional histogram equalization can be used on each region to correct for non-uniform illumination. For this, we utilize the human visual system to segment the image, using the measure of image enhancement to select $\alpha 2$ and $\alpha 3$. The first three images are then equalized separately and unionized, with the remaining pixels filled in. In summary, the algorithm is executed as follows:

Input Image

Step 1: Segment image using Human Vision Thresholding algorithm

Step 2: Equalize images 1, 2, and 3 separately

Step 3: Recombine the pixels in the three equalized images

Step 4: Fill in the missing pixels

Output Image

4. COMPUTER SIMULATIONS

In this section, we present the results of computer simulations. The proposed method has been tested using a variety of images, including uniformly illuminated, well and poorly illuminated, and non-uniformly illuminated, and images with shadows. The test images include images that were produced by high-quality professional digitization methods as well as lower quality cell phone cameras.

We compare against the results of other leading histogram equalization methods. The comparison is made both by visual inspection and the Logarithmic AME performance measure. The results show the proposed method to produce more visually pleasing enhanced images and more consistently produce optimal enhanced images.

Figure 2 shows the resulting images for the bed image. As can be seen from visual inspection, the proposed algorithm creates the most visually pleasing enhanced image. It corrects for the largely under-illuminated scene, allowing details such as the bed and pictures to be seen clearly. Further, properly illuminated details such as the light and the image in the window can still be seen clearly.

Figure 3 shows the resulting images for a camera phone image. The original image, in figure 3.a, has regions of under-illumination, over-illumination, and proper illumination. The enhanced images using bi-histogram equalization only enhance one section, making either the under-illuminated background visible or correcting the over-illuminated foreground. The image in figure 3.f, using the proposed method, corrects both regions such that all areas of the image can be clearly seen.

Figure 4 summarizes the results for a representative range of images, showing the results of the quantitative measure for the enhanced images. As can be seen from the

(a) (b) (c) (d)

Figure 2: Bed image enhanced using the variants of histogram equalization; (a)Original bed image, bed image enhanced using (b)recursive mean-separate histogram equalization, (c)brightness preserving histogram equalization with maximum entropy (d)human vision based multi-histogram equalization

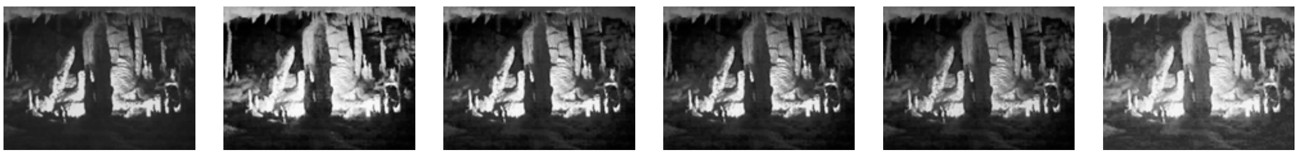

(a) (b) (c) (d) (e) (f)

Figure 3: Cave image enhanced using the variants of histogram equalization; (a)Original cave image, cave image enhanced using (b)dualistic sub-image histogram equalization, (c)minimum mean brightness error bi-histogram equalization, (d)recursive mean-separate histogram equalization, (e)brightness preserving histogram equalization with maximum entropy, (f) human vision based multi-histogram equalization

numbers, the proposed algorithm consistently outperforms the other histogram equalization algorithms.

Image	HVSMHE	DSHE	MMBEBHE	RMSHE	BPHEME
bed	973.8	1006	1007	1006	991.8
cave	277.1	222.8	178.2	178.8	189.3
faces	641.2	530.4	449.0	475.9	454.7
street	237.2	159.2	128.6	139.1	135.9
school	635.6	442.7	372.7	353.6	417.9

Figure 4: Logarithmic AME results for the proposed algorithm and other equalization methods

5. CONCLUSION

In this paper we introduced a new method for performing histogram equalization, resulting in a more robust histogram equalization that is able to correct images with regions of over-illumination, under-illumination, and proper illumination. We compared the results of the proposed algorithm to the results of the leading histogram equalization methods. The effectiveness of the proposed method was shown both visually and quantitatively. This demonstrates that the Multi-Histogram Equalization method using HVT is effective for the enhancement of images with regions of improper illumination.

6. REFERENCES

[1] Y. Wang, Q. Chen, B. Zhang, "Image Enhancement Based on Equal Area Dualistic Sub-Image Histogram Equalization Method," IEEE Transactions on Consumer Electronics, vol. 45, no. 1, pp. 68-75, Nov. 1998.

[2] S.D. Chen, A.R. Ramli, "Contrast Enhancement using Recursive Mean-Separate Histogram Equalization for Scalable Brightness Preservation", IEEE Transactions on Consumer Electronics, vol. 49, no. 4, pp. 1301-1309, Nov. 2003.

[3] S.D. Chen, A.R. Ramli, "Minimum Mean Brightness Error Bi-Histogram Equalization in Contrast Enhancement," IEEE Transactions on Consumer Electronics, vol. 49, no. 4, pp. 1310-1319, Nov. 2003.

[4] C. Wang, Z. Ye, "Brightness Preserving Histogram Equalization with Maximum Entropy: A Variational Perspective," IEEE Transactions on Consumer Electronics, vol. 51, no. 4, pp. 1326-1334, Nov. 2005.

[5] A.M. Vossepoel, B.C. Stoel, A.P. Meershoek, "Adaptive Histogram Equalization Using Variable Regions," in Proc. IEEE Conference on Pattern Recognition, Rome, pp. 351-353, Nov. 1988.

[6] M. Jourlin, J.C. Pinoli, "Logarithmic Image Processing; The Mathematical and Physical Framework for the Representation and Processing of Transmitted Images," Advances in Imaging and Electron Physics, vol. 115, pp. 129-196, 2001.

[7] E. Wharton, S. Agaian, K. Panetta, "Comparative Study of Logarithmic Enhancement Algorithms with Performance Measure," in Proc. SPIE Electronic Imaging, San Jose, CA, #6064 12, Jan. 2006.

[8] E. Wharton, S. Agaian, K. Panetta, "A Logarithmic Measure of Image Enhancement," in Proc. SPIE Defense and Security Symposium, Orlando, FL, #62500P, Apr. 2006.